Journal of Biomedical Optics 8(3), 357–361 (July 2003)

Spectroscopic approach for monitoring two-photon excited fluorescence resonance energy transfer from homodimers at the subcellular level

Vickie J. LaMorte*
University of California
Beckman Laser Institute
Laser Microbeam and Medical Program
Irvine, California 92612
E-mail: lamorte@bli.uci.edu

Aikaterini Zoumi
University of California
Beckman Laser Institute
Laser Microbeam and Medical Program
Irvine, California 92612
and
University of California
Department of Biomedical Engineering
Irvine, California 92612

Bruce J. Tromberg
University of California
Beckman Laser Institute
Laser Microbeam and Medical Program
Irvine, California 92612
and
University of California
Department of Biomedical Engineering
Irvine, California 92612

Abstract. We have employed a spectroscopic approach for monitoring fluorescence resonance energy transfer (FRET) in living cells. This method provides excellent spectral separation of green fluorescent protein (GFP) mutant signals within a subcellular imaging volume using two-photon excited fluorescence imaging and spectroscopy (TPIS-FRET). In contrast to current FRET-based methodologies, TPIS-FRET does not rely on the selection of optical filters, ratiometric image analysis, or bleedthrough correction algorithms. Utilizing the intrinsic optical sectioning capabilities of TPIS-FRET, we have identified protein–protein interactions within discrete subcellular domains. To illustrate the applicability of this technique to the detection of homodimer formation, we demonstrated the *in vivo* association of promyleocyte (PML) homodimers within their corresponding nuclear body.
[DOI: 10.1117/1.1584052]

Keywords: two-photon imaging and spectroscopy; fluorescence resonance energy transfer; promyelocyte protein; homodimers; green fluorescent protein.

Paper MM-02 received Oct. 17, 2002; revised manuscript received Jan. 14, 2003; accepted for publication Jan. 15, 2003.

1 Introduction

A myriad of proteins found to interact *in vitro* has raised the issue of demonstrating the occurrence of these direct interactions *in vivo* and more specifically, their spatial localization within discrete cellular domains. The advent of green fluorescent protein (GFP) fluorophores has prompted the utilization of fluorescence resonance energy transfer (FRET) to monitor protein–protein interaction.[1–3] In FRET, direct excitation of a donor molecule results in nonradiative energy transfer to an acceptor molecule, provided the molecules are within approximately 10 to 100 Å of each other.[4,5] For efficient FRET, the emission spectrum of the donor must sufficiently overlap with the excitation spectrum of the acceptor molecule. While traditionally FRET has been used to calculate intra- and intermolecular distances between two sites,[3,6] determination of the occurrence of a protein–protein interaction relies mainly on whether FRET is observed, since this process occurs within the Förster distance.[7]

Recent studies employing spectrally overlapping GFP mutants and FRET methods to identify protein–protein interactions have relied extensively on utilization of optical filters to separate the donor's fluorescence from that of the acceptor's fluorescence followed by intensity-based ratiometric imaging.[2,8] Major obstacles have been encountered with these approaches and are not limited to distinguishing the FRET signal from simple donor and acceptor fluorescence spectral overlap and accounting for differences in expression levels of the donor and acceptor molecules. This has introduced ambiguities in the interpretation of a FRET signal[2,3] and has largely limited the utilization of FRET to monitoring inducible cellular protein interactions.[9–11] Here, the donor intensity image in the absence of FRET is obtained from the sample to perform intensity-based ratiometric image analysis. A ratiometric measurement requires approximately equal levels of donor and acceptor expression from cell to cell, typically relying on the creation of multiple, stably transfected cell lines, careful selection of optical filters, and the development of advanced algorithms to minimize spectral bleedthrough. Alternative approaches to quantitatively monitoring FRET have been based on fluorescence lifetime imaging and donor photobleaching.[3,12,13]

Two-photon excited fluorescence microscopy relies on the simultaneous absorption of two near-infrared photons to cooperatively excite an electronic transition equivalent to that obtained by single-photon, ultraviolet excitation followed by fluorescence emission.[14] Two-photon excited fluorescence imaging is advantageous over its single-photon counterpart for monitoring protein dynamics, such as FRET, in living cells owing to its intrinsic optical sectioning capability, which minimizes photobleaching and photodamage.[15,16] Identification of the FRET signal still relies on filters and ratiometric image analysis. In contrast to imaging approaches, spectral acquisition negates the need for filters and ratiometric mea-

*Author to whom correspondence should be addressed; V.J.L. and A.Z. contributed equally to this work.

1083-3668/2003/$15.00 © 2003 SPIE

surements, and facilitates quantification of the individual components of the FRET signal.

Detection of noninducible homodimerization versus heterodimerization is inherently more difficult since at most only 50% of the dimers will contribute to the FRET signal. Furthermore, dimers formed exclusively by a donor or acceptor obscure the FRET signal. The promyleocyte (PML) has been shown to localize to discrete nuclear bodies[17] whose function remains unclear. Its dissociation from these bodies and participation in a chromosomal translocation with the retinoic acid receptor α (RARα) are hallmarks for acute promyelocytic leukemia (APL). Dimerization of PML has been demonstrated *in vitro* to be mediated by the coiled-coil domain of the protein, which is also responsible for the heterodimerization between PML and the fusion protein PMLRARα in APL.[18] To this end, we chose to investigate the formation and subcellular spatial distribution of PML homodimers *in vivo*. We demonstrate that integration of two-photon excited fluorescence microscopy, spectral acquisition, and second-generation GFP mutants enable the detection of PML homodimers in subcellular domains in the living cell.

2 Experimental Protocol

2.1 *Plasmid Construction*

CFP (Clontech, Palo Alto, California) and YFP (Topaz) (Packard BioSciences, Meriden, Connecticut) mutants were subcloned C-terminally into a CMV-driven expression plasmid containing the PML sequence as previously described.[19] Specifically, both GFP mutants were generated by a polymerase chain reaction (PCR) using the respective plasmids as a template and oligos containing an Mlu1 site at the 5′ end and an Xba1 site at the 3′ end. The fragments were inserted into the CMX-PML vector that was digested with Mlu1 and Nhe1 at the C-terminal. For control experiments, pCDNA3-NLS-ECFP, containing a nuclear localization signal (a gift from Drs. B. Forman and C. Solier) was subcloned from the pCDNA3-NLS-ECFP-RARα expression plasmid,[9] (a gift from Dr. C. Glass).

2.2 *Cell Culture and Microinjection*

HEp-2 cells (ATCC, Manassas, Virginia) were cultured as previously described[19] in drilled 35-mm dishes with an alphanumerically gridded coverslip (Bellco Glass, Vineland, New Jersey) affixed to the bottom. Approximately 10^{-15} liters/cell of DNA plasmid (50 ng/μl) were introduced into the nucleus of the cell using a semiautomated microinjection system (Eppendorf Scientific, Westbury, New York) and a Zeiss Axiovert microscope (Zeiss Inc., Oberkochen, Germany). The DNA plasmid concentration was kept equal for CFP and YFP to ensure equivalent expression within a cell. The cells were incubated overnight before FRET analysis to permit expression.

2.3 *Two-Photon Imaging and Spectroscopy System*

The two-photon imaging microscope used for this study has been described[20] and has been modified to include a SpectraPro-150 spectrograph. Briefly, it consists of a modelocked Ti:sapphire laser (170-fs pulse width, 76-MHz repetition rate; Mira 900F, Coherent, Santa Clara, California) pumped by a 5-W Verdi laser (Coherent). The beam exiting

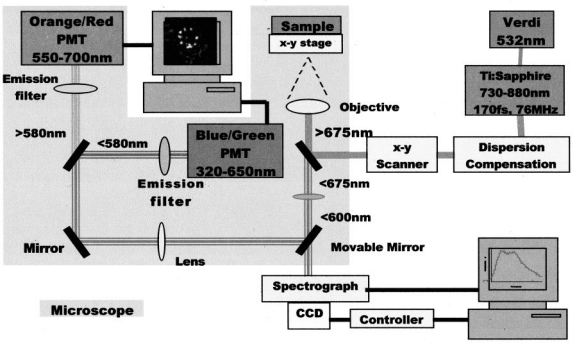

Fig. 1 Diagram of the two-photon imaging and spectroscopy system.

the laser is deflected into the back port of an inverted Axiovert 100 microscope (Zeiss Inc.) and scanned across the sample via a personal computer (PC) controlled galvanometer-driven x-y scanner (Series 603X, Cambridge Technology, Watertown, Massachusetts). The beam is reflected by a short-pass 675-nm dichroic beamsplitter (Chroma Technology Corp., Brattleboro, Vermont) and focused onto the sample with a 63×, c-apochromat, NA = 1.2, water immersion microscope objective (Zeiss Inc.). For NLS-CFP control experiments, a 100×, NA = 1.45 oil immersion microscope objective (Zeiss Inc.) was used. The average power entering the microscope is approximately 30 mW (2.5 mW at the sample site). Two-photon excited fluorescence from the sample is epicollected, discriminated with the dichroic beamsplitter, filtered by a short-pass 600-nm filter (CVI Laser Corp., Livermore, California) and detected. Two-dimensional (x-y plane) images (256×256 pixels) are acquired at a rate of 1 frame/s (pixel dwell time of 16 μs/pixel) with a single-photon counting photomultiplier tube (PMT) (Hamamatsu Corp., Bridgewater, New Jersey) and cover an area of 35×35 μm for the 63× microscope objective. An SBG39 wide-pass (322 to 654-nm) blue-green emission filter (CVI Laser Corp., Albuquerque, New Mexico) is placed in front of the PMT. Spectra are obtained with a SpectraPro-150 spectrograph equipped with a 300 grooves/mm grating blazed at 500 nm (Acton Research Corp., Acton, Massachusetts), and a high dynamic range MicroMax:512BFT CCD camera (Princeton Instruments, Trenton, New Jersey), which is controlled by an ST-133 Controller (Princeton Instruments). The spectrograph and camera settings are PC-controlled through commercially available software (WinSpec/32 v. 2.4.6.6, Roper Scientific Inc., Trenton, New Jersey). The CCD temperature is maintained at the minimum possible temperature (−45 °C) for all the experiments to ensure low dark noise. The entrance slit of the spectrograph is set to a width of 0.5 mm. The spectral acquisition time was 60 s. For the NLS-CFP control, the spectral acquisition time was 10 s. Switching between imaging and spectral acquisition is achieved by changing the position of a built-in microscope mirror. When both two-photon images and spectra are acquired from the sample, the two-photon images are acquired and stored; this is immediately followed by acquisition of emission spectra from the same depth (z) into the sample. Autofluorescence of the cell is negligible. Dark noise spectra are subtracted from the acquired sample spectra.

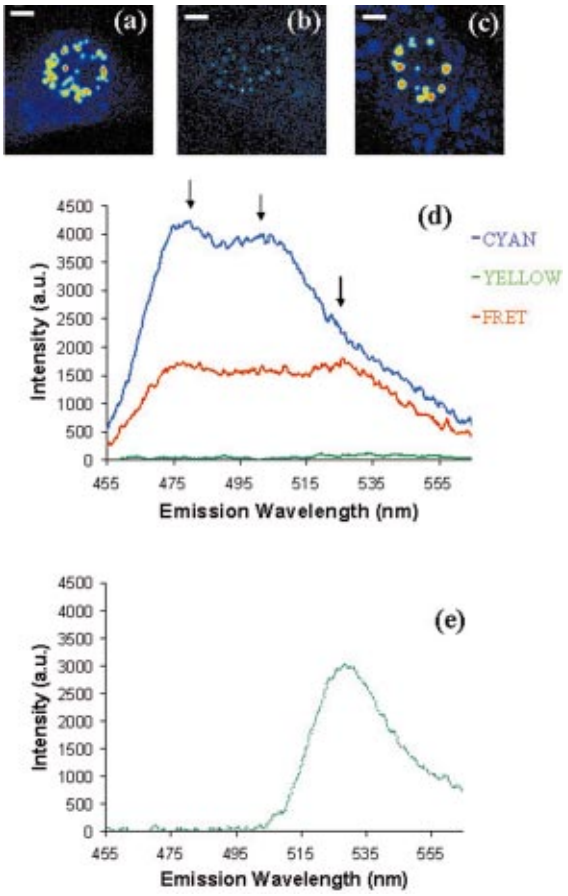

Fig. 2 Two-photon excited fluorescence image of (a) PMLCFP, (b) PMLYFP, and (c) PMLCFP/PMLYFP (FRET) with corresponding emission spectra (d) for an excitation wavelength of 810 nm. (e) Two-photon emission spectrum of PMLYFP for an excitation wavelength of 866 nm. The images depict an optical section of the PML nuclear bodies within the nucleus. Minimal excitation of the acceptor is apparent in both the image and the emission spectra for PMLYFP. Peak excitation values are indicated with arrows (↓) at 476, 501, and 527 nm, and the ratios were calculated from corresponding intensity values. Scale bar equals 3 μm.

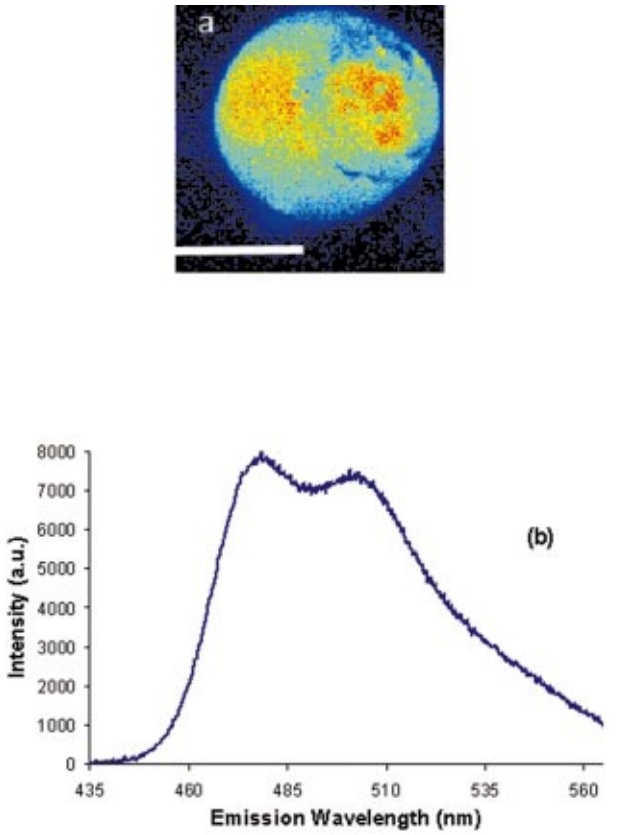

Fig. 4 Two-photon excited fluorescence image (a) of NLSCFP/PMLYFP (FRET) with corresponding emission spectra (b) for an excitation wavelength of 810 nm. The image shows an optical section of the CFP fluorescence localized to the nucleus. The ratios were calculated from corresponding intensity values at 476, 501, and 527 nm. The average ratio values for 527/476 nm and 501/476 nm for twelve cells expressing the donor and the acceptor (NLSCFP/PMLYFP) were 0.52 ± 0.01 and 0.95 ± 0.003, respectively. An unpaired Student's *t*-test analysis for the 501/476-nm ratios was not statistically significant ($p = 0.1036$), reflecting the consistency of this ratio for donor (CFP) fluorescence. An unpaired Student's *t*-test analysis of the 527/476-nm ratios was not significant ($p = 0.6076$), which is indicative of the absence of FRET. Scale bar equals 10 μm.

2.4 *Data Analysis*

Acquired 256×256 pixel images were converted to bitmap format with no postprocessing modifications. Spectral data were imported into Microsoft Excel 2000 (Microsoft Corp.) and plotted with intensity (arbitrary units) versus the emission wavelength (nanometers). Because of the low signal-to-noise ratio in the acceptor alone case, a moving average (period: 20) function was used to plot the spectra. Peak intensity ratios were statistically analyzed (Instat, San Diego, California) by an unpaired Student's *t*-test, and a probability value was calculated.

3 Results and Discussion

Plasmids encoding fusion proteins of PML with either a donor, CFP (Clontech), or an acceptor, YFP or Topaz (Packard BioSciences), were introduced alone or in combination into HEp-2 cells (ATCC). Two-photon images of cells expressing the donor (PMLCFP) alone, the acceptor (PMLYFP) alone, and both (PMLCFP/PMLYFP) were acquired with a two-photon imaging and spectral detection system (Fig. 1) at an excitation wavelength of 810 nm. This wavelength was selected for its minimal excitation of the acceptor, which is a crucial requirement for the detection of FRET.[8] Other wavelengths tested throughout the tuning range of the Ti:sapphire laser (730 to 880 nm) exhibited efficient, direct excitation of the acceptor (YFP). Subsequent to single-scan image acquisition, the emission spectrum from the same optical section was collected at a 60-s acquisition time. Images of one representative cell out of ten examined cells for a single experiment are presented for each case. To ensure reproducibility of the results, experiments were performed in triplicate.

Two-photon excited fluorescence images [Figs. 2(a), 2(b), and 2(c) (see color plate)] depict the subcellular localization of the PML fusion proteins to nuclear bodies as previously reported.[19] As evident in Fig. 2(b), the fluorescence signal of the acceptor protein (PMLYFP) is minimal. In contrast, the donor (PMLCFP) alone and the combination (PMLCFP/PMLYFP) are efficiently excited [Figs. 2(a) and 2(c)]. The standard approach of ratioing the FRET to donor images for determination of FRET is not reliable here since the expression levels of the proteins may vary between different optical sections within the bodies and from cell to cell. Furthermore, since a decrease in the donor fluorescence intensity is observed in the presence of FRET compared with the donor alone, image ratioing may overcorrect the FRET response. The two-photon emission spectrum of CFP [Fig. 2(d), blue] covers a region from 450 to 580 nm, with maxima at 476 and 501 nm. When YFP is efficiently excited at 866 nm, its emission spans a region from 510 to 580 nm, with a maximum at 527 nm [Fig. 2(e)]. Maximal two-photon excitation of YFP is not feasible owing to the limitations imposed by the tuning range of the laser (730 to 880 nm). The *in vivo* spectra (Fig. 2) are consistent with the *in vitro* spectra obtained from purified GFPs.[2] Control studies were performed and demonstrated that prolonged irradiation (>9 min) of the sample did not alter the recorded image or spectral intensities as expected owing to the photostability of CFP.[21] As expected in FRET, a decrease in CFP intensity was observed in the donor–acceptor spectrum [Fig. 2(d), red], with a concomitant increase in YFP intensity compared with the individual spectra for the donor [Fig. 2(d), blue] and the acceptor [Fig. 2(d), green] alone.

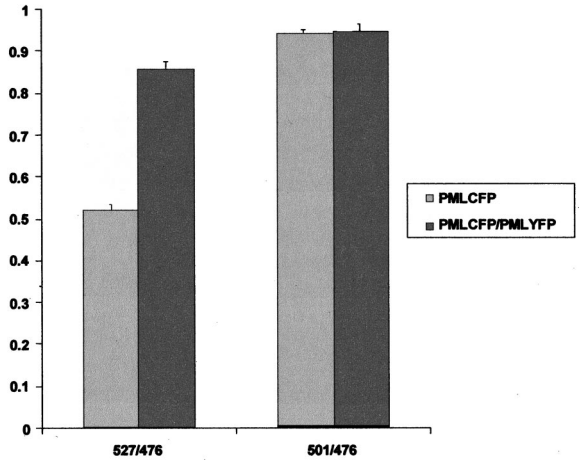

Fig. 3 Average ratio values for 527/476 nm and 501/476 nm. The ratio values for ten cells expressing the donor alone (PMLCFP) were 0.52 ± 0.01 and 0.94 ± 0.002 for 527/476 nm and 501/476 nm, respectively. The ratio values for ten cells expressing the donor and the acceptor (PMLCFP/PMLYFP) were 0.86 ± 0.02 and 0.95 ± 0.01, respectively. The ratios are independent of expression levels from cell to cell. An unpaired Student's *t*-test analysis for the 501/476-nm ratios was not statistically significant ($p = 0.773$), reflecting the consistency of this ratio for donor (CFP) fluorescence. An unpaired Student's *t*-test analysis of the 527/476-nm ratios was highly significant ($p < 0.0001$), indicating a statistical difference between donor and donor–acceptor cells, revealing the occurrence of FRET.

To further illustrate the occurrence of FRET between CFP and YFP, the ratio of intensity of the 527-nm peak to that of the 476-nm peak was calculated for cells expressing the donor alone and for those expressing the FRET pair. In the presence of CFP alone, this ratio is consistently 0.52. For the 810-nm two-photon excitation, YFP intensity values at 527 nm are negligible for the acceptor alone. Thus, an increase in the 527/476-nm ratio in cells expressing both CFP and YFP would serve as a measure of FRET occurrence, which would be indicative of a protein–protein interaction. The 501/476-nm ratio corresponds to CFP expression only and serves as a spectral fingerprint for CFP whether expressed alone or in combination with YFP. Inherent to the spectra of CFP, this ratio is preserved at 0.9 irrespective of changes in expression levels between cells.

As described earlier, ratios were calculated for individual cells expressing PMLCFP and those expressing PMLCFP/PMLYFP, and the average ratio values are presented in Fig. 3. The average of the 501/476-nm ratio was 0.94 ± 0.002 and 0.95 ± 0.01, for PMLCFP and PMLCFP/PMLYFP, respectively. The average of the 527/476-nm ratios was 0.52 ± 0.01 and 0.86 ± 0.02 for PMLCFP and PMLCFP/PMLYFP, respectively. An unpaired Student's *t*-test analysis for the 501/476-nm ratios was not statistically significant ($p = 0.773$) reflecting the consistency of this ratio for donor (CFP) fluorescence. An unpaired Student's *t*-test analysis of the 527/476-nm ratios was highly significant ($p < 0.0001$) indicating a statistical difference between donor and donor–acceptor cells. The observed increase in the 527/476-nm ratio is a direct result of the energy transfer between CFP and YFP and reveals a protein–protein interaction in PML homodimers.

As a negative control, NLSCFP, which contains a nuclear localization signal and directs CFP to the nucleus, was introduced into cells as the donor. PMLYFP was maintained as the acceptor. Figure 4(a) (see color plate) depicts the two-photon fluorescence image of a cell expressing NLSCFP/PMLYFP at 810-nm excitation with fluorescence distributed throughout the nucleus. The corresponding spectrum [Fig. 4(b)] has two peaks at 476 and 501 nm. The 527/476-nm ratio for NLSCFP/PMLYFP is 0.52 ± 0.01, which is identical to that measured for the donor alone (0.52 ± 0.01), indicating the absence of FRET. The 501/476-nm ratio for NLSCFP/PMLYFP was 0.95 ± 0.003, which is consistent with donor-alone values.

Monitoring FRET by two-photon imaging and spectroscopy uniquely enables the examination of protein–protein interactions at the subcellular level. It reveals for the first time the localization and formation of PML homodimers within the corresponding nuclear bodies *in vivo*. These findings open new avenues of exploration into the dynamics of PML and the proteins that reside within these bodies, which in turn will provide new insight into the function of the PML body. The TPIS-FRET method can be extended to other cellular questions that focus on protein interactions that may occur within discrete domains, such as transcription. Temporal and spatial resolution of these interactions can be achieved by this approach, which inherently provides structural and functional information from subfemptoliter volumes.

TPIS-FRET is advantageous over ratiometric analysis for the qualitative determination of FRET because it negates the need for postprocessing of the images and the utilization of optical filters. It is independent of protein expression levels from cell to cell, and transiently transfected or microinjected DNA expression plasmids can be readily evaluated. This spectroscopic technique should be applicable to other mutant GFP pairs. It invites future analysis of engineered protein–protein interactions in tissue by exploiting the ability of near-infrared light to penetrate deeply into living tissue.

Understanding the function of a protein by following its dynamic interplay with other proteins in a living cell can contribute fundamentally to understanding the overall cellular process or disease in which it participates. Future studies will examine spatial and temporal variations of PML interactions with other proteins, including PMLRARα, within living cells and tissues.

Acknowledgments

The authors gratefully acknowledge the contributions of Tatiana B. Krasieva, Gopi Manthripragada, Jessica Lee, Timothy Osborne, Shrimati Datta, Barry M. Forman, Corinne Solier, Christopher Glass, and Michael Berns to this work. This work was supported by National Institutes of Health grant P41RR01192 and a grant from the National American Heart Association to VJL (993005N).

References

1. R. Y. Tsien, ''The green fluorescent protein,'' *Annu. Rev. Biochem.* **67**, 509–544 (1998).
2. B. A. Pollok and R. Heim, ''Using GFP in FRET-based applications,'' *Trends Cell Biol.* **9**, 57–60 (1999).
3. P. R. Selvin, ''The renaissance of fluorescence resonance energy transfer,'' *Nat. Struct. Biol.* **7**, 730–734 (2000).
4. T. Förster, ''Delocalized excitation and excitation transfer,'' in *Modern Quantum Chemistry*, pp. 93–137, Academic Press, New York (1965).
5. L. Stryer, ''Fluorescence energy transfer as a spectroscopic ruler,'' *Annu. Rev. Biochem.* **47**, 819–846 (1978).
6. A. Y. Louie and B. J. Tromberg, ''Fluorescence energy resonance energy transfer: FRET studies of ligand binding to cell surface receptors,'' *J. Fluorescence* **8**, 13–20 (1998).
7. J. R. Lakowicz, *Principles of Fluorescence Spectroscopy*, 2nd ed., Kluwer Academic/Plenum, New York (1999).
8. A. Periasamy, ''Fluorescence resonance energy transfer microscopy: a mini review,'' *J. Biomed. Opt.* **6**, 287–291 (2001).
9. J. Llopis, S. Westin, M. Ricote, J. Wang, C. Y. Cho, R. Kurokawa, T. M. Mullen, D. W. Rose, M. G. Rosenfeld, R. Y. Tsien, and C. K. Glass, ''Ligand-dependent interactions of coactivators steroid receptor coactivator-1 and peroxisome proliferator-activated protein with nuclear hormone receptors can be imaged in live cells and are required for transcription,'' *Proc. Natl. Acad. Sci. U.S.A.* **97**, 4363–4368 (2000).
10. K. Prufer, A. Racz, G. C. Lin, and J. Barsony, ''Dimerization with retinoid X receptor promotes nuclear localization and subnuclear targeting of vitamin D receptors,'' *J. Biol. Chem.* **275**, 41114–41123 (2000).
11. R. Y. Tsien and A. Miyawaki, ''Seeing the machinery of live cells,'' *Science* **280**, 1954–1955 (1998).
12. T. W. J. Gadella and T. M. Jovin, ''Oligomerization of epidermal growth factor receptors on A431 cells studied by time-resolved fluorescence imaging microscopy. A stereochemical model for tyrosine kinase receptor activation,'' *J. Cell Biol.* **129**, 1543–1558 (1995).
13. A. G. Harpur, F. S. Wouters, and P. I. H. Bastiaens, ''Imaging FRET between spectrally similar GFP molecules in single cells,'' *Nat. Biotechnol.* **19**, 167–169 (2001).
14. W. Denk, J. H. Strickler, and W. W. Webb, ''Two-photon laser scanning fluorescence microscopy,'' *Science* **248**, 73–76 (1990).
15. A. Periasamy, ''Localization of protein interactions in a single living cell: Two-photon excitation FRET microscopy,'' *Microscopy and Microanal* (in press).
16. M. G. Xu, B. Crimeen, M. J. Ludford-Menting, X. Gan, S. M. Russell, and M. Gu, ''Three-dimensional localization of fluorescence resonance energy transfer in living cells under two-photon microscopy,'' *Scanning* **23**, 9–13 (2000).
17. J. A. Dyck, G. G. Maul, W. H. Miller, J. D. Chen, A. Kakizuka, and R. M. Evans, ''A novel macromolecular structure is a target of the promelocyte-retinoic acid receptor oncoprotein,'' *Cell* **76**, 333–343 (1994).
18. P. Kastner, A. Perez, Y. Lutz, C. Rochette-Egly, M. P. Gaub, B. Durand, M. Lanotte, R. Berger, and P. Chambon, ''Structure, localization and transcriptional properties of two classes of retinoic acid receptor alpha fusion proteins in acute promyelocytic leukemia (APL): structural similarities with a new family of oncoproteins,'' *EMBO J.* **11**, 629–642 (1992).
19. V. J. LaMorte, J. A. Dyck, R. L. Ochs, and R. M. Evans, ''Localization of nascent RNA and CBP with the PML-containing nuclear body,'' *Proc. Natl. Acad. Sci. U.S.A.* **95**, 4991–4996 (1998).
20. A. K. Dunn, V. P. Wallace, M. Coleno, M. W. Berns, and B. J. Tromberg, ''Influence of optical properties on two-photon fluorescence imaging in turbid samples,'' *Appl. Opt.* **39**, 1194–1201 (2000).
21. M. Elangovan, R. N. Day, and A. Periasamy, ''Nanosecond fluorescence resonance energy transfer-fluorescence lifetime imaging microscopy to localize the protein interactions in a single living cell,'' *J. Microsc.* **205**, 3–14 (2002).